

Electronic Supplementary Information:
**Ultrafast hole relaxation between dual valence bands in
methyllummonium lead iodide**

Sen Mou,^{1,*} Mauro Leoncini,² Salvatore Macis,³ Luca Tomarchio,³
Gabriele Nisticò,³ Annalisa D'Arco,¹ Maria Chiara Paolozzi,³ Massimo
Petrarca,⁴ Salvatore Gambino,² Aurora Rizzo,² and Stefano Lupi^{3,5}

¹*INFN and Physics Department, University of Rome "La Sapienza",
P.le Aldo Moro 5, 00185 Rome, Italy*

²*CNR NANOTEC – Istituto di Nanotecnologia,
c/o Campus Ecotekne, Via Monteroni, 73100 Lecce, Italy*

³*Physics Department, University of Rome "La Sapienza",
P.le Aldo Moro 5, 00185 Rome, Italy*

⁴*INFN and SBAI, Department of Basic and Applied Sciences for Engineering,
University of Rome "La Sapienza", Via Scarpa 16, 00161 Rome, Italy*

⁵*INFN-LNF, Via E. Fermi 40, 00044 Frascati, Italy*

* msengz@163.com

I. COMPLEX FREQUENCY-RESOLVED PHOTOCONDUCTIVITY

The complex frequency-resolved THz photoconductivity can be extracted from experimental data with the following formula[1]

$$\Delta\sigma(\omega) = -\frac{n+1}{Z_0 \times d} \frac{\Delta E(\omega, t_{pp})}{E_{ref}(\omega)} \quad (S1)$$

The following Drude-Lorentz model can be employed to describe the complex frequency-resolved THz photoconductivity.[2]

$$\Delta\sigma(\omega, t_{pp}) = \sigma_{DS}(\omega, t_{pp}) + \Delta\sigma_{TO}(\omega, t_{pp}) - i\varepsilon_0\omega\Delta\varepsilon_\infty \quad (S2)$$

where $\Delta\varepsilon_\infty$ represents the photoinduced change in the background dielectric constant, σ_{DS} describes the conductivity of photoinduced carriers.

$$\sigma_{DS}(\omega, t_{pp}) = \varepsilon_0\omega_p^2 \frac{\tau}{1-i\omega\tau} \left(1 + \frac{C}{1-i\omega\tau}\right) \quad (S3)$$

where τ is the scattering time. Parameter C ($-1 \leq C \leq 0$) indicates the localisation of carriers: $C=-1$ and 0 , respectively, indicate completely localised and Drude-limit free carriers. ω_p is plasma frequency and can be expressed as:

$$\omega_p = \sqrt{\frac{e^2 N}{\varepsilon_0 m^*}} \quad (S4)$$

where e is the charge of an electron, N is the density of the carriers, and m^* is the effective mass of the carrier.

Assuming no photoinduced change of the damping rate, $\Delta\sigma_{TO}(\omega, t_{pp})$ is the first-order differential to the Lorentzian function of equation (2) in the main text, which is employed to describe the photo modulation of the two phonon modes.[2]

$$\Delta\sigma_{TO}(\omega, t_{pp}) = \sum_{m=1}^2 \left\{ \frac{2\varepsilon_0\omega_{p,m}\omega}{i(\omega_m^2 - \omega^2) + \omega\gamma_m} \Delta\omega_{p,m} + \frac{-2i\omega_m\varepsilon_0\omega_{p,m}^2\omega}{[i(\omega_m^2 - \omega^2) + \omega\gamma_m]^2} \Delta\omega_m \right\} \quad (S5)$$

where $\Delta\omega_{p,m}$ and $\Delta\omega_m$ are the change of the phonon oscillator strength and the phonon frequency shift.

As shown in Fig. S1, the model described by equation (S2) well reproduces the experimental frequency-resolved complex photoconductivity for the pump at 800 nm. The contribution of photocarriers to the photoconductivity, described by the Drude-Smith model,

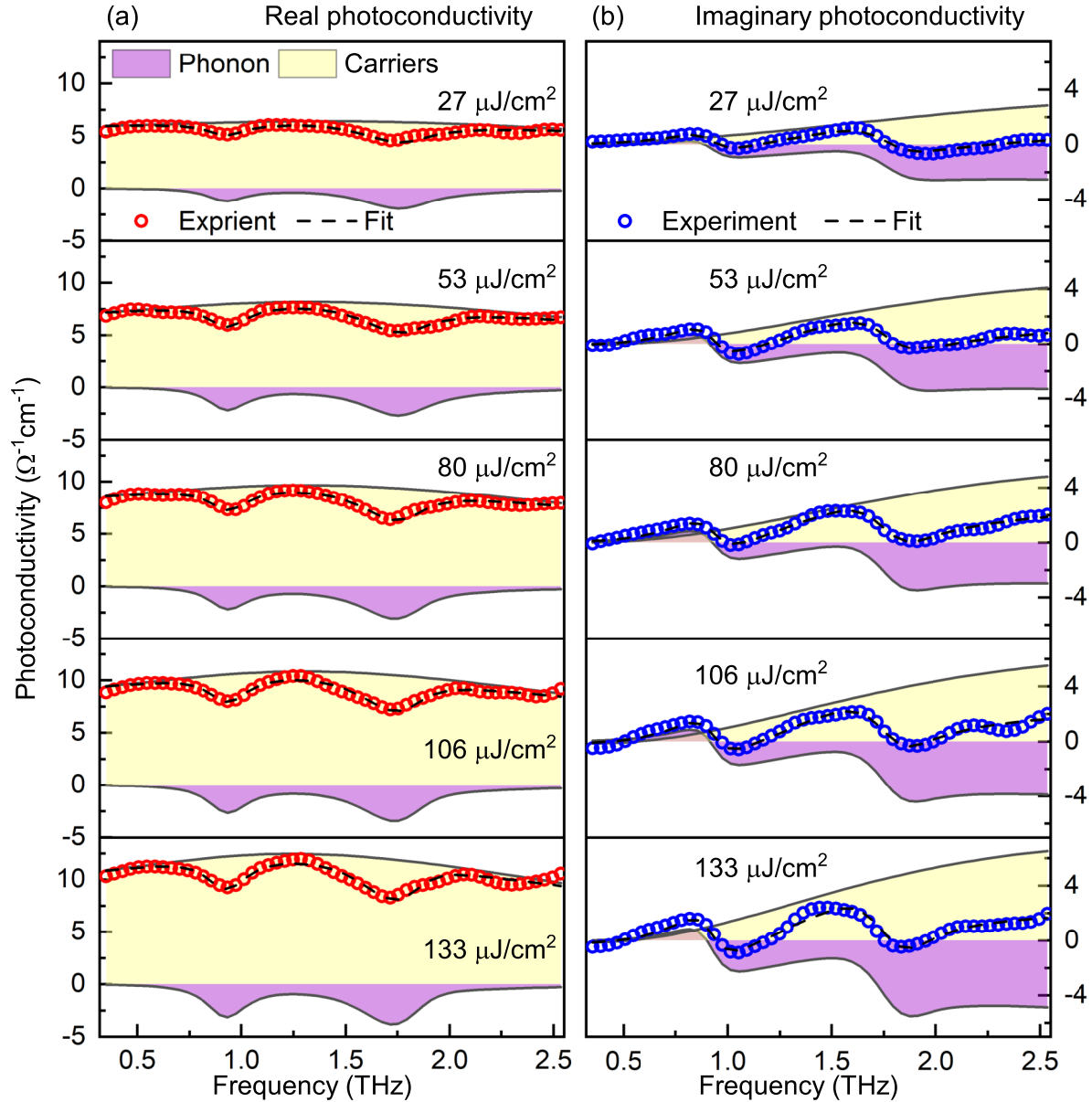


Figure S1. Frequency-resolved THz photoconductivity with pump at 800 nm. (a) The real part of the complex THz photoconductivity. (b) The imaginary part of the complex THz photoconductivity. The experimental photoconductivity is decomposed into two components, respectively, resulting from the photocarriers and the interaction between the photocarriers and phonons. The Drude-Smith model is applied to describe the photoconductivity from the photocarriers, while the first-order differential to two Lorentzian functions is employed to describe the photocarrier-phonon interactions. The increasing pump fluence enhances both the contributions from the photocarriers and the photocarrier-phonon interactions.

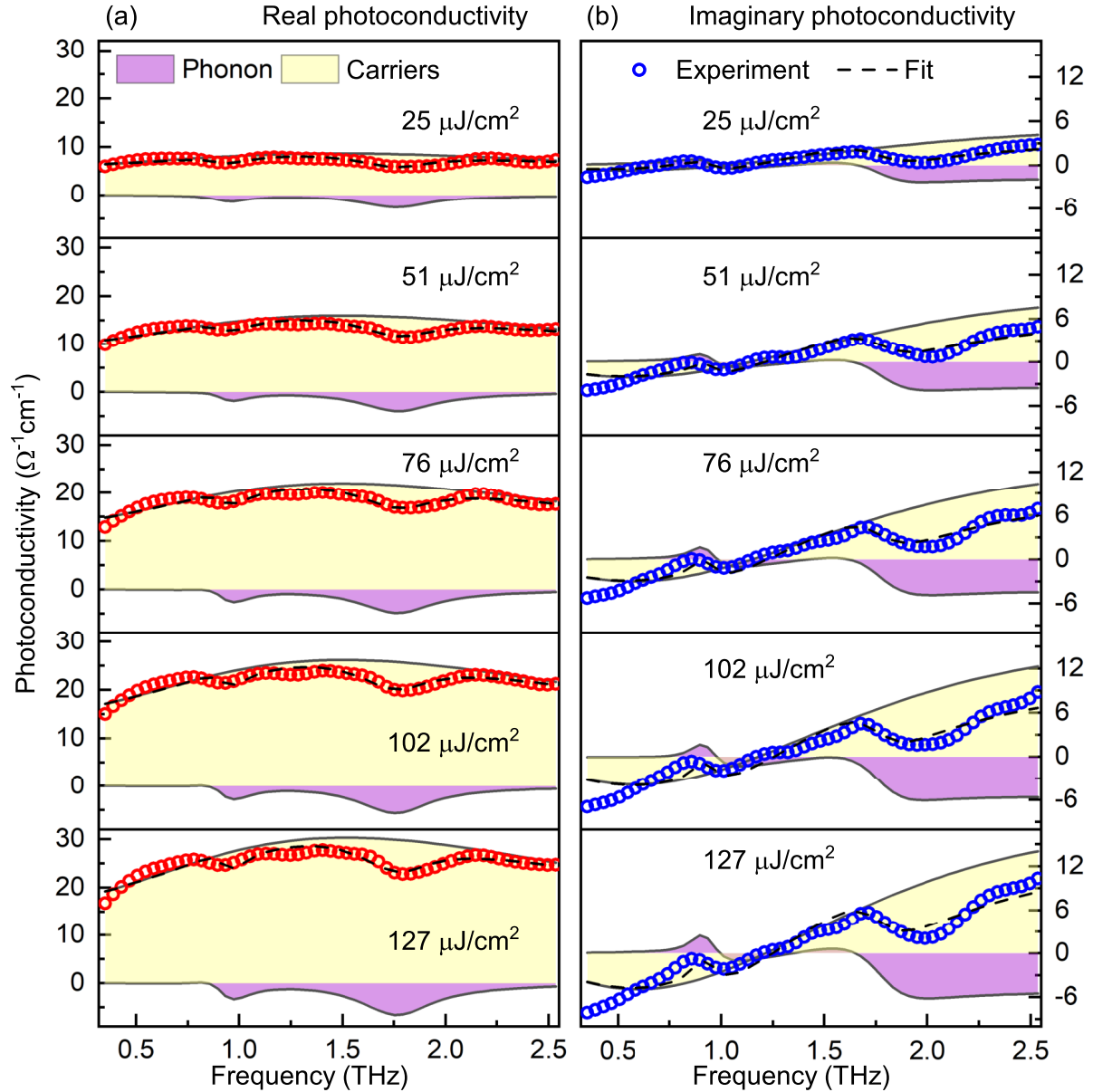


Figure S2. Frequency-resolved THz photoconductivity with pump at 400 nm. (a) The real part of the complex THz photoconductivity. (b) The imaginary part of the complex THz photoconductivity. The experimental photoconductivity is decomposed into two components resulting from photocarriers and the interaction between photocarriers and phonons. The Drude-Smith model and the first-order differential to two Lorentzian functions describe the photoconductivity from the photocarriers and the photocarrier-phonon interactions. The increasing pump fluence enhances both the contributions from the photocarriers and the photocarrier-phonon interactions.

increases with the increasing pump fluence. In addition, the photo modulation of the two phonon modes is enhanced by increasing pump fluence. Similar behaviour is observed for the photoconductivity with the pump at 400 nm, which is presented in Fig. S2.

The same model reproduces the experimental complex frequency-resolved photoconductivity with a pump at 400nm. As the pump fluence increases, the photoconductivity increases, and the interaction between the photocarriers and phonons is also enhanced.

II. FITTING PARAMETERS FOR THE CONDUCTIVITY DECAY

The black solid curves in Fig. 6 in the main text are obtained by fitting the experimental data with eqn. (4). The fitting parameters and their confidence intervals are presented in table I. When the sample is excited with the pump at 800 nm, only a slow exponential component is necessary to reproduce the experimental data. Instead, fast and slow exponential components must be used to fit the experimental data when the sample is excited at 400 nm. The decay constant τ_f increases with the pump fluence, and the constant τ_s decreases with the pump fluence.

TABLE I: Fitting parameters for the conductivity decay and their confidence intervals.

The errors represent statistical errors at a confidence level of 68% (one sigma).

Wavelength (nm)	Fluence ($\mu\text{J}/\text{cm}^2$)	A_f	$\tau_f(ps)$	A_s	$\tau_s(ns)$
800	27	n/a	n/a	1.93 ± 0.01	3.64 ± 0.10
	51	n/a	n/a	2.14 ± 0.01	3.58 ± 0.09
	76	n/a	n/a	3.01 ± 0.01	2.88 ± 0.05
	102	n/a	n/a	3.40 ± 0.01	2.51 ± 0.04
	127	n/a	n/a	3.88 ± 0.01	2.14 ± 0.02
400	25	0.17 ± 0.05	15.0 ± 6.6	3.12 ± 0.01	3.08 ± 0.08
	51	1.10 ± 0.03	31.0 ± 1.5	5.39 ± 0.01	1.76 ± 0.01
	76	2.25 ± 0.02	44.4 ± 1.0	6.84 ± 0.01	1.45 ± 0.01
	102	3.02 ± 0.02	57.0 ± 0.9	7.55 ± 0.01	1.41 ± 0.01
	127	3.95 ± 0.02	57.8 ± 0.8	8.14 ± 0.01	1.33 ± 0.01

III. ESTIMATION OF CARRIER DENSITY

The carrier density can be calculated with the following equation[3]

$$n_0 = \frac{F[1 - \exp(-\alpha d)]}{E_{ph}d} \quad (\text{S6})$$

where n_0 is the carrier density, F represents the pump fluence, α denotes the absorption coefficient, d stands for the thickness of the sample, and E_{ph} is the photon energy. The efficiency of the conversion from photons to carriers is assumed to be 100%. The sample thickness is 400 nm.

-
- [1] J. K. Gustafson, P. D. Cunningham, K. M. McCreary, B. T. Jonker, and L. M. Hayden, Ultrafast carrier dynamics of monolayer ws2 via broad-band time-resolved terahertz spectroscopy, *J. Phys. Chem. C* **123**, 30676 (2019).
- [2] D. Zhao, H. Hu, R. Haselsberger, R. A. Marcus, M.-E. Michel-Beyerle, Y. M. Lam, J.-X. Zhu, C. La-o vorakiat, M. C. Beard, and E. E. M. Chia, Monitoring electron–phonon interactions in lead halide perovskites using time-resolved thz spectroscopy, *ACS Nano* **13**, 8826 (2019).
- [3] H. Okochi, H. Katsuki, M. Tsubouchi, R. Itakura, and H. Yanagi, Photon energy-dependent ultrafast photoinduced terahertz response in a microcrystalline film of ch3nh3pbbr3, *J. Phys. Chem. Lett.* **11**, 6068 (2020).